Spry1 and Spry2 are necessary for eyelid closure

Murali R. Kuracha[1], **Ed Siefker**[1], **Jonathan D. Licht**[2], and **Venkatesh Govindarajan**[1],[@]

[1]Department of Surgery, 2500 California Plaza, Creighton University, Omaha, NE 68178

[2]Division of Hematology/Oncology, Feinberg School of Medicine, Northwestern University, Chicago, Illinois

Abstract

Sproutys (Sprys) are downstream targets and negative feedback regulators of the FGF-Ras-ERK signaling pathway. Our previous studies have shown that Spry1 and Spry2, through negative modulation of FGF-ERK signaling, allow lens vesicle separation from the overlying ectoderm and regulate corneal epithelial proliferation. Here we show that Spry1 and Spry2 are necessary for eyelid closure. Murine palpebral conjunctival epithelial cells that differentiate as inner eyelids and adjacent mesenchymal cells express *Spry1* and *Spry2* prior to eyelid closure. Conditional deletion of both *Spry1* and *Spry2*, but not either one alone, in the ocular surface epithelial cells result in the "EOB" (eyes open at birth) phenotype suggesting redundant roles for these proteins during eyelid closure. Spry mutant eyelids show increased proliferation of conjunctival epithelial cells with concomitant induction of FGF targets, *Erm*, *Pea3* and *Dusp6* and elevated ERK phosphorylation. Peridermal cells at the leading edge of Spry-mutant eyelids showed reduced c-Jun, but not ERK, phosphorylation, reduced F-actin polymerization and reduced motility in vitro. Spry mutant eyelids also showed disruptions in epithelial mesenchymal interactions reflected in the enhanced mesenchymal *Spry1* and *Spry4* expression, disaggregation of *BMP4*-positive mesenchymal cells and loss of Shh in the eyelid epithelium. Spry mutant eyelids also showed increased Wnt signaling and reduced expression of *Foxc1* and *Foxc2*, two transcription factors previously shown to be necessary for eyelid closure. Collectively, our results show that conjunctival epithelial Spry1 and Spry2 redundantly promote eyelid closure by a) stimulating ERK-independent, c-Jun-mediated peridermal migration, b) suppressing conjunctival epithelial proliferation through FGF-ERK signaling, c) mediating conjunctival epithelial-mesenchymal interactions and d) maintaining expression of *Foxc1* and Foxc2.

Keywords

eyelids; Sprouty; FGF; ERK; c-Jun; Wnt; Foxc1; Foxc2

Introduction

The eyelid anlagen are specified by embryonic day 9 (E9) (Swindell et al., 2008). Eyelids become morphologically distinct by E11.5 with the invagination of the dorsal and ventral portions of the ocular surface ectoderm adjacent to the globe. The palpebral conjunctival

Publisher's Disclaimer: This is a PDF file of an unedited manuscript that has been accepted for publication. As a service to our customers we are providing this early version of the manuscript. The manuscript will undergo copyediting, typesetting, and review of the resulting proof before it is published in its final citable form. Please note that during the production process errors may be discovered which could affect the content, and all legal disclaimers that apply to the journal pertain.

epithelium lines the inner surface and palpebral epidermis lines the outer surface of the eyelid enclosing loosely organized mesenchymal cells. The palpebral conjunctival epithelium is contiguous with the bulbar conjunctival epithelium which in turn, is contiguous with the corneal epithelium. After E11.5, peridermal cells at the leading edges of the upper (dorsal) and lower (ventral) eyelids migrate toward each other to initiate eyelid closure. Fusion of the two leading edges is complete by E15.5. The eyelids remain closed until post natal day 14 (P14) at which time they reopen. Other adnexal organs that arise from the conjunctival epithelia include goblet cells that contribute mucus secretions to the tear film and meibomian and lacrimal glands that contribute lipid and aqueous secretions to the tear film respectively.

A number of genes including growth factors (FGF10, TGF-α, HB-EGF) (Luetteke et al., 1993; Mine et al., 2005; Tao et al., 2005), growth factor receptors (FGFR2, BMPR1a, EGFR) (Li et al., 2001; Luetteke et al., 1994; Miettinen et al., 1995; Vassalli et al., 1994), cytoplasmic effectors (MAP3K1, SMAD4, JNK) (Huang et al., 2009; Takatori et al., 2008; Zhang et al., 2003) and transcription factors (c-Jun, Foxc1, Foxc2) (Li et al., 2003; Smith et al., 2000; Zenz et al., 2003) have been shown to regulate eyelid growth and closure. Germline or conditional deletion of these genes in the ocular surface epithelial cells alter growth and result in the EOB phenotype. In particular, perturbations in FGF and BMP signaling profoundly alter eyelid growth and differentiation. FGF10, expressed in the eyelid mesenchyme and its cognate receptor, FGFR2, expressed in the conjunctival epithelial cells are necessary for eyelid closure (Tao et al., 2005). Downstream of FGFR2, BMP4-SMAD4 mediated signaling has been shown not only to control epithelial growth but also to maintain conjunctival cell fate (Huang et al., 2009). Conditional deletion of SMAD4 in the epithelial cells results in a switch from conjunctival to epidermal differentiation program and keratinization of the ocular surface epithelia. The sensitivity of eyelid epithelial cells to growth factor signaling suggests the possibility of positive and negative feedback mechanisms that would allow precise modulation of signaling strength in these cells. Whether such feedback mechanisms exist has not been explored.

Sproutys have been shown to be direct targets and negative feedback regulators of fibroblast growth factor (FGF) signaling in invertebrates and in vertebrates (Chambers and Mason, 2000; Faedo et al., 2010; Hanafusa et al., 2002; Minowada et al., 1999). Four members of the Sprouty family, Spry1–4, have been identified. Of these, Spry3 is expressed in the adult brain and testes but not in the embryo (Minowada et al., 1999). Loss of function studies in mice show that Spry1 and Spry2 play critical roles during early development of multiple organ rudiments including kidney (Basson et al., 2005; Basson et al., 2006), inner ear (Shim et al., 2005), tooth (Klein et al., 2006) and cortical patterning in the brain (Faedo et al., 2010). More recently, we have shown that Spry1- and Spry2-mediated negative modulation of FGF-ERK signaling regulates lens vesicle separation and corneal epithelial proliferation (Kuracha et al., 2011). In this study, by conditional deletion of *Spry1* and *Spry2* in the ocular surface epithelial cells, we show that these genes also promote eyelid closure through FGF-ERK-mediated regulation of conjunctival epithelial proliferation and ERK-independent, c-Jun-mediated peridermal cell migration.

Material and Methods

Generation of *Spry1^{fl/fl}; Spry2^{fl/fl}; Cre* Mice

Spry1 and *Spry2* floxed mice (Basson et al., 2005; Klein et al., 2006) were crossed to Le-Cre transgenic mice (Ashery-Padan et al., 2000) to delete *Spry1* and *Spry2* in the ocular surface epithelial cells as described previously (Kuracha et al., 2011). Matings were set up such that Cre-positive embryos or pups were hemizygous for the Cre transgene. Recombination and

excision of *loxP* flanked sequences in *Spry1* and *Spry2* genes were confirmed as described previously (Kuracha et al., 2011).

Histological Analyses

Timed pregnancies were set up and pregnant females were sacrificed at appropriate time points. Spry mutant offspring were identified by PCR as described previously (Kuracha et al., 2011). Heads of Spry mutant and control heads were harvested, fixed in 10% formalin, embedded in paraffin, sectioned frontally and stained with hematoxylin and eosin.

In situ Hybridization

In situ hybridization was performed as described previously using ^{35}S-UTP-labelled riboprobes (Kuracha et al., 2011). *Spry1*, *Spry2*, *cyclin D1*, *cyclin D2*, *Erm*, *Pea3*, *Cre* and *Dusp6* were synthesized as described previously (Kuracha et al., 2011). The *BMP4* antisense probe was synthesized using *Eco*RI-digested *BMP4* cDNA and SP6 RNA polymerase. The *Shh* antisense probe was synthesized using *Eco*RI-digested *Shh* cDNA and T7 RNA polymerase. The *Foxc1* antisense probe was synthesized using *Pst*I-digested *Foxc1* cDNA and T7 RNA polymerase. The *Foxc2* antisense probe was synthesized using *Pst*I-digested *Foxc2* cDNA and T7 RNA polymerase. The *Axin2* antisense probe was synthesized using *Eco*RI-digested *Axin2* cDNA and T3 RNA polymerase. The *sFRP* antisense probe was synthesized using *Pst*I-digested *sFRP* cDNA and T7 RNA polymerase. The *K4* antisense probe was synthesized using *Spe*I-digested *K4* cDNA and T7 RNA polymerase. Bright- and dark-field images were captured separately using an Eclipse E600 microscope (Nikon, Tokyo, Japan). Silver grains in the dark-field images were pseudocolored red using Adobe Photoshop CS3 (Adobe systems, San Jose, CA) and overlaid on corresponding bright-field images.

Immunohistochemistry

Immunohistochemistry (IHC) on formalin-fixed paraffin embedded sections was performed as described previously (Kuracha et al., 2011). Sections were mounted using anti-fade medium containing DAPI (ProLong; Invitrogen, Carlsbad, CA). In figures where IHC data are shown, antigen-antibody complexes are red, and nuclei are stained blue with DAPI.

Proliferation Assay

BrdU incorporation assay was performed to measure cell proliferation as described previously (Kuracha et al., 2011). Quantification of cell proliferation (BrdU labeling index) was performed by calculating the fraction of BrdU positive nuclei over the total number of nuclei for each section. Sections from a minimum of three different embryos were analyzed from control and Spry mutants for each time point. Analysis was performed by student's t test by comparing *Spry* mutant and *Cre-* samples at P 0.05 (Prism 5, GraphPad, La Jolla, CA).

Isolation and Culturing Primary Keratinocytes

Isolation and culture of primary keratinocytes was performed as described by Li et al. (Li et al., 2003) with minor modifications. Eyelids of new born mice were dissected, rinsed in 1X PBS and incubated in solution containing dispase (MP Biologicals, IN), at 4°C overnight. The dermis was separated from epidermis with forceps and minced in 0.25% trypsin EDTA for 5 minutes to generate a single cell suspension. These cells were then cultured in a mouse keratinocyte culture medium containing defined keratinocyte-serum free media (KSFM) (GIBCO BRL) supplemented with 10 ng/ml EGF.

In Vitro Scratch Assay

To analyze eyelid epithelial cell motility, Spry mutant and Cre- primary keratinocytes were seeded onto six well plate or chamber slides (BD Biosciences), grown to confluence and transferred to a growth factor-free medium containing mitomycin C (Sigma) and cultured for a day. The confluent monolayer was then wounded by a disposable pipette tip (Fisher), washed once with 1X PBS to remove the floating cells and fresh defined KSFM containing 10 ng/ml EGF was added back to the culture. Images were captured immediately and 48 hours later. The number of cells that migrated into the gap after 48 hours was counted. For immunostaining, cells were washed twice with PBS and fixed in 4% formaldehyde solution in PBS for 10 minutes at room temperature. Alexa 488 conjugated phalloidin (Molecular Probes) was used to stain F-actin.

RESULTS

Spry1, Spry2 and *Spry4* expression in the eyelid precursor cells

Spry1, *Spry2* and *Spry4* expression prior to (E12.5, E14.5) and during (E15.5) eyelid closure was analyzed by in situ hybridization (Fig. 1). As both upper (dorsal) and lower (ventral) eyelids showed similar patterns of expression for these three genes, only lower eyelid expression is shown in Fig. 1. At E12.5, when the ocular surface ectoderm invaginates to form the presumptive eyelids, the palpebral conjunctival epithelial cells expressed *Spry1* and *Spry2* (Fig. 1A, B) but not *Spry4* (Fig. 1C). Palpebral (Fig. 1A, B, white arrows) and forniceal epithelial cells (Fig. 1A, B, green arrows) showed stronger expression of *Spry1* and *Spry2* than bulbar epithelial cells. A similar expression pattern was seen in the conjunctival epithelial cells at E14.5 and E15.5 (Fig. 1D, E, G, H, white arrows). At E12.5, mesenchymal cells adjacent to the conjunctival epithelia expressed *Spry2* and *Spry4* (Fig. 1B, C). Later, at E14.5 and at E15.5, eyelid mesenchymal cells expressed all three *Sprys* (Fig. 1D–I′). Of these, Spry1 expression was stronger in the mesenchymal cells closer to the margin (Fig. 1D, G, G′, green arrows). The presumptive eyelid epidermis expressed *Spry1* and *Spry2* at E14.5 and E15.5 (Fig. 1D, E, G, H, magenta arrows) and *Spry4* at E15.5 (Fig. 1I, magenta arrow). During eyelid closure at E15.5, peridermal cells at the leading edge expressed all three *Sprys* (Fig. 1G′–I′, yellow arrows). Thus, *Spry* expression in the eyelid precursor cells during epithelial invagination and peridermal migration suggested regulatory roles for these genes during eyelid differentiation and morphogenesis.

Sprys are required for eyelid closure

To test the hypothesis that Sprys are necessary for eyelid differentiation, we deleted *Spry1* and *Spry2* in the ocular surface epithelial cells by Cre-mediated recombination and excision of *Spry1* and *Spry2* floxed alleles (Fig. 1J–L). Cre recombinase expression was driven by the Pax6 promoter (Le-Cre) that is active by E9 in the lens placode and ocular surface ectoderm (Ashery-Padan et al., 2000). We confirmed Cre recombinase expression in the palpebral and bulbar conjunctival epithelial cells by in situ hybridization (Fig. 1J, white arrows). Cre expression was also noted in the presumptive eyelid epidermis (Fig. 1J, magenta arrow). *Spry1* (Fig. 1K, arrows) and *Spry2* (Fig. 1L, arrows) expression in the *Spry1^{fl/fl}*; *Spry2^{fl/fl}*; Cre (will be referred to as Spry CKO) conjunctival epithelial and eyelid epidermal cells was substantially reduced confirming Cre-mediated excision of *Spry1* and *Spry2*. Interestingly, spry4 expression in the palpebral conjunctival epithelial cells was modestly increased in the Spry CKO eyelids (Fig. 1 compare M to F). Also, the mesenchymal cells adjacent to the bulbar and palpebral conjunctival epithelia expressed higher levels of all three *Sprys* (Fig. 1 compare K to D, L to E and M to F). These results suggested profound perturbations in eyelid epithelial-mesenchymal interactions upon loss of *Spry1* and *Spry2* in the epithelial cells.

Loss of two alleles of *Spry1* or *Spry2* or three alleles of *Spry1* and *Spry2* did not show any abnormalities in eyelid development (Supplementary Fig. 1) suggesting that *Spry1* or *Spry2* was dispensable for eyelid differentiation. But loss of all four alleles of *Spry1* and *Spry2* (Spry CKO) resulted in the EOB phenotype (Fig. 2A, B, arrows). Histological analysis did not reveal alterations in eyelid morphology prior to E14.5. The Spry CKO palpebral conjunctival epithelium was thickened prior to (E14.5), during (E15.5) and after (E16.5) eyelid closure (Fig. 2D′, F′, H′, red arrows). Pronounced thickening of palpebral epidermis was noticeable at E16.5 (Fig. 2H′, magenta arrow). At E15.5, the peridermal cells at the leading edges of the upper and lower eyelids in the control (Cre-) embryos had migrated to initiate eyelid closure (Fig. 2E′, arrows) and by E16.5, the margins of the two eyelids had fused (Fig. 2G′, arrow). In contrast, the Spry CKO peridermal cells at the dorsal and ventral margins had not migrated towards the middle of the eye at E15.5 (Fig. 2F, arrows) or at E16.5 (Fig. 2H, arrows). The Spry CKO eyelids remained unfused at P1 (Fig. 2J, J′, black arrows) and infiltration of inflammatory cells between the open eyelids were seen (Fig. 2J, J′, asterisk). Fewer hair follicles were noted in the Spry CKO eyelids (Fig. 2I′, J, red arrows). These data suggested that the EOB phenotype in the Spry CKO mice is due to a failure of eyelid closure rather than premature opening of eyelids and that Spry1 and Spry2 function redundantly to regulate eyelid closure. In this article, we report changes in the eyelid differentiation program. Alterations in the development of other organ rudiments derived from the conjunctival epithelia including meibomian glands, lacrimal and Harderian glands were also seen but are not reported here.

Increased proliferation of Spry CKO eyelid epithelia

To assess whether the conjunctival hyperplasia in Spry CKO embryos was due to increased cell proliferation, BrdU incorporation assays were performed (Fig. 3A–E). Quantification of the BrdU labeling index revealed a statistically significant increase in palpebral conjunctival proliferation of the upper and lower eyelids and in bulbar conjunctival proliferation of the lower eyelids (Fig. 3A–E). Consistent with these results, *cyclin D1* expression was increased in the palpebral conjunctival epithelial cells of the upper (Fig. 3F, G) and lower eyelids (Fig. 3H, I). *Cyclin D2*, in contrast, was more strongly expressed in the bulbar epithelial cells, particularly in the lower eyelids (Fig. 3J–M). Peridermal epidermis and eyelid mesenchymal cells adjacent to the conjunctival epithelia did not show a statistically significant difference in proliferation (data not shown). No alterations in active caspase 3 immunoreactivity were observed in Spry CKO eyelids at E12.5, E14.5 or E15.5 (data not shown) excluding cell death as a possible cause for the observed phenotype. These results suggested that the Spry CKO conjunctival hyperplasia was due to increased proliferation.

Increased FGF signaling in Spry CKO embryos

The ETS domain transcription factors, Erm and Pea3, and the MAP kinase phosphatase *Dusp6* (MKP3) have been shown to be downstream targets of FGF signaling (Kawakami et al., 2003; Li et al., 2007; Sharrocks, 2001). As Sprys negatively regulate FGF signaling, we assessed alterations in FGF signaling in Spry CKO eyelids by analyzing *Erm*, *Pea3* and *Dusp6* expression (Fig. 4). At E14.5, the Spry CKO palpebral conjunctival epithelial cells showed increased expression of *Erm*, *Pea3* and *Dusp6* (Fig. 4A–F, white arrows). The bulbar conjunctival epithelial cells and the palpebral epidermis also showed strong expression of *Erm* (Fig. 4B, teal and magenta arrows). The peridermal cells at the eyelid margins showed increased expression of *Erm* and *Pea3* and to a lesser extent, *Dusp6* (Fig. 4A–F). No differences in expression were seen between upper and lower eyelids. Similar results were seen at E12.5 (Supplementary Fig. 2). These results suggested that Spry1 and Spry2 negatively regulate FGF signaling in the eyelid epithelia prior to eyelid closure. Interestingly, *Erm* was also induced in the Spry CKO eyelid mesenchymal cells (Fig. 4B) consistent with induction of *Spry1* and *Spry4*, two other targets of FGF signaling, in these

same cells (Fig. 1L, M). Together, these results suggest an increase in FGF signaling in the Spry CKO eyelid mesenchymal cells.

Decreased phospho-c-Jun and increased ERK activity in Spry CKO eyelids

c-Jun expression and phosphorylation in the migrating peridermal cells at the leading edge have been shown to be necessary for eyelid closure (Li et al., 2003). Alterations in c-Jun phosphorylation in Spry CKO eyelids were assessed by immunohistochemistry (Fig. 5A–D ′). In Spry CKO eyelids, there were fewer peridermal cells with phosphorylated c-Jun (Fig. 5A–D′, arrows). The palpebral and bulbar conjunctival cells in contrast, did not show a substantial difference in phospho-c-Jun levels (data not shown). As Sprys can increase ERK phosphorylation downstream of FGF signaling, we assessed alterations in ERK phosphorylation in Spry CKO eyelids (Fig. 5E–H″). The bulbar and conjunctival epithelial cells of the Spry CKO eyelids (Fig. 5F″, H″, white arrows) but not the peridermal cells (Fig. 5F′, H′, yellow arrows), showed increased ERK phosphorylation. ERK phosphorylation in the eyelid mesenchymal cells was comparable to controls (Fig. 5E–H). These results correlated reduced peridermal migration to decreased c-Jun phosphorylation and increased conjunctival proliferation to enhanced ERK phosphorylation.

BMP4 and *Shh* expression in Spry CKO eyelids

As previous studies have shown that FGF10-FGFR2 signaling is necessary for BMP4 and Shh expression in the eyelid primordia (Huang et al., 2009; Tao et al., 2005), we analyzed the expression of these two genes in Spry CKO eyelids (Fig. 6A–D′). In the control eyelids, *BMP4* expression was localized to a cluster of mesenchymal cells near the margin (Fig. 6A, A′, white arrows) that were immediately adjacent to *Shh*-positive cells in the palpebral conjunctival epithelium (Fig. 6C, C′, arrows). The *Shh* expression domain marks the region where the eyelash rudiment will form (Tao et al., 2005). In the Spry CKO eyelids, a broader domain of *BMP4* expression was seen in the mesenchymal cells (Fig. 6B, white arrows) and the compact, clustered organization of *BMP4* positive cells seen in the control eyelids was not seen. Condensation of *BMP4*-positive mesenchymal cells in the skin epidermal hair follicle rudiment appeared unaltered (Fig. 6B, green arrows). Coincidentally, *Shh* expression was decreased in the Spry CKO palpebral conjunctival cells (Fig. 6D, D′, arrows). These data support the notion of disrupted epithelial-mesenchymal communication in the Spry CKO eyelids. Interestingly, in the Spry CKO conjunctival epithelial cells, phosphorylation of SMAD2 and SMAD1/5/8, two downstream effectors of BMP signaling, were not decreased in Spry CKO eyelids (Supplementary Fig. 3). These data would suggest that the disaggregation of BMP4-positive mesenchymal cells is of little functional consequence in altering SMAD-mediated signaling in the epithelial cells. Consistent with these results, alterations in conjunctival differentiation or a switch from conjunctival to epidermal fate as seen in the SMAD4 conditional null eyelids were not seen (assessed by K10, K14, and K4 expression) (Supplementary Fig. 4).

Foxc1 and *Foxc2* expression in Spry CKO eyelids

The forkhead transcription factors, *Foxc1* and *Foxc2*, have been shown to be critical for eyelid differentiation (Smith et al., 2000). Expression of *Foxc1* and *Foxc2* in Spry CKO eyelids were analyzed by in situ hybridization (Fig. 7). In the control eyelids, the conjunctival epithelial cells near the margin and the peridermal leading edge cells expressed *Foxc1* and *Foxc2* (Fig. 7A, A′, C, C′, white and yellow arrows). In the Spry CKO eyelids, the conjunctival cells near the anterior margin showed a modest reduction in *Foxc1* (Fig. 7B, B′, white arrows) and a stronger reduction in *Foxc2* (Fig. 7D, D′, white arrows). The Spry CKO peridermal cells showed reduced *Foxc1* and *Foxc2* expression (Fig. 7B′, D, D′, yellow

arrows). These results suggested that conjunctival *Foxc1* and *Foxc2* expression depends on signaling mediated by Sprys.

Altered expression of Wnt signaling components in Spry CKO eyelids

Excessive Wnt signaling inhibits eyelid closure (Gage et al., 2008; Mukhopadhyay et al., 2006). Also, increased Wnt signaling in the FGFR2-null conjunctival epithelial cells has been reported (Huang et al., 2009). These results suggest an inverse correlation between Wnt and FGF signaling in the eyelids. To assess alterations in Wnt signaling, we examined expression of *Axin2* and *sFRP*, a target and antagonist of Wnt signaling respectively (Fig. 8). Spry CKO conjunctival epithelial cells near the margin showed a modest reduction in *Axin2* expression (Fig. 8A–B′, white arrows). In contrast, *sFRP* expression was increased in the palpebral and bulbar conjunctival epithelial cells (Fig. 8C–D′, arrows). Axin2 expression was reduced in Spry CKO mesenchymal cells (Fig. 8B, B′) but appeared unaltered in the palpebral epidermis (Fig. 8A, B, magenta arrows). These results suggested that increased FGF signaling due to loss of Sprys correlated with decreased Wnt signaling in the eyelid epithelial cells.

Slower migration of Spry CKO eyelids peridermal cells

To test the hypothesis that Spry CKO eyelid fail to close due to impaired motility of peridermal cells, we performed scratch assays using eyelid keratinocytes from Spry CKO and Cre- embryos (Fig. 9A–E). Cre-mediated deletion and excision of *Spry1* and *Spry2* alleles in these cells was confirmed by PCR (Supplementary Fig. 5). 48 hours after the scratch was made, fewer Spry CKO keratinocytes had migrated into the gap (Fig. 9D, E) indicating a reduced capacity for migration. Spry CKO keratinocytes also showed reduced phalloidin (binds F-actin) staining (Fig. 9G, I). Peridermal cells in the Spry CKO embryos also showed a consistent reduction in phallodin staining at the leading edge (Fig. 9J–M, arrows). These results suggested that the impaired motility of Spry CKO peridermal cells is likely due to reduced actin polymerization and stress fiber formation.

In summary, our results show that deletion of *Spry1* and *Spry2* in the ocular surface epithelial cells leads to the following; a) failure of eyelid closure, b) increased proliferation of conjunctival epithelial cells with increased expression of *cyclin D1* and *cyclin D2*, c) induction of FGF signaling targets in the conjunctival epithelial cells, d) decreased phosphorylation of c-Jun in the peridermal cells and increased phosphorylation of ERKs in the conjunctival epithelial cells, e) reduction in Shh expression in the anterior eyelids with loss of clustering of *BMP4*-positive mesenchymal cells, f) reduction in *Foxc1* and *Foxc2*, g) decreased expression of Wnt signaling target, *Axin2* and increased expression of Wnt antagonist, *sFRP* in the conjunctival epithelial cells and h) decreased motility, reduction in actin stress fibers and reduced F-actin polymerization in peridermal cells.

Discussion

Deletion of *Spry1* and *Spry2* in the ocular surface ectodermal cells did not affect the formation of eyelid rudiments in their proper locations or invagination of eyelid epithelial precursors suggesting that *Spry1* and *Spry2* were dispensable for eyelid fate specification and invagination. Our data instead suggest roles for Sprys in coordination of morphogenetic events that control eyelid closure.

Failure of eyelid closure in the Spry CKO embryos is likely due to the following; a) reduced migration of peridermal cells, b) increased proliferation of conjunctival epithelial cells and c) disrupted signaling interactions between conjunctival epithelium and adjacent mesenchyme (Fig. 10). Though our data supports a), b) and c), reduced peridermal motility

is likely to be the most direct and proximal cause for inhibition of eyelid closure. The slower motility in turn, is likely to be due to reduced c-Jun phosphorylation, F actin polymerization and stress fiber formation as these events have been shown to be critical drivers of peridermal migration (Geh et al., 2011; Takatori et al., 2008). How do Sprys regulate c-Jun phosphorylation? It is possible that Sprys modulate the signaling cascade upstream of c-Jun phosphorylation that includes MEKK1 (MAP3K) and JNK activation. Alternatively, Sprys could regulate signaling initiated by growth factors active in this area such as FGF10, HB-EGF or TGFα and that aberrant activation of these signaling pathways could lead to c-Jun activation. Enhanced FGF signaling in the leading edge peridermal cells partially supports this hypothesis. Interestingly, this increase in FGF signaling is ERK-independent.

A second reason for failure of eyelid closure in Spry CKO embryos could be the increased proliferation of conjunctival epithelial cells. Concomitant with this increase in proliferation was the induction of a) *cyclins D1* and *D2*, b) Erk phosphorylation and c) downstream targets of FGF signaling targets including *Erm*, *Pea3* and *Dusp6*. These results suggest that Sprys, through mediation of the FGF-ERK pathway, suppress conjunctival epithelial proliferation. The FGF pathway targeted is likely to be initiated by FGF10 and its receptor, FGFR2 (Fig. 10). The eyelid mesenchymal cells express FGF10 prior to eyelid closure (Ohuchi et al 2005). Germline deletion of FGF10 results in decreased proliferation of conjunctival epithelial cells and failure of eyelid closure. Conditional deletion of FGFR2 in the ocular surface ectoderm also inhibits eyelid closure. These results considered together would suggest that Sprys through negative modulation of FGF10-FGFR2 signaling, control conjunctival epithelial proliferation. Just as decreased proliferation, excessive proliferation of conjunctival epithelial cells also appears to be detrimental to eyelid closure. This would suggest that a critical function of Spry is to act as a negative feedback regulator of FGF signaling to suppress ectopic growth. These results, considered together with our previously published data that show increased proliferation of Spry CKO corneal epithelial cells (Kuracha et al., 2011) supports the notion that the main function of Sprys in the ocular surface epithelial cells is to act as 'fine tuners' of growth factor signaling.

A third reason for lack of eyelid closure in Spry CKO embryos could be due to disrupted communication between the conjunctival epithelium and adjacent mesenchyme. Alterations in expression of *Shh* in the epithelial cells, *Spry1*, *Spry2* and *Spry4* in the mesenchymal cells and disaggregation of *BMP4*-positive mesenchymal cells reflect alterations in eyelid epithelial-mesenchymal interactions. Some of these changes such as the localized loss of epithelial Shh expression are likely to be more relevant to the growth and development of specific organ rudiments (eyelash, meibomian glands) in the anterior regions of the eyelids. Still, indirect effects of these altered signaling interactions on eyelid closure cannot be ruled out. These data also support the notion that reciprocal signaling between eyelid epithelium and underlying mesenchyme is sensitive to alterations in FGF signaling.

Huang et al show that conditional deletion of FGFR2 in the conjunctival cells results in increased Wnt signaling, extra row of hair follicles (distichiasis) and inhibition of eyelid closure (Huang et al., 2009). These results are complemented by our studies that show that increased FGF signaling in Spry CKO eyelids leads to a reduction in Wnt signaling (reduced *Axin2* and increased *sFRP*). But ectopic hair follicles were not seen in the conjunctival epithelia. *Foxc2* (a target of Wnt signaling in the eyelid epithelia) was reduced but not completely extinguished. This residual expression of *Foxc2* may explain at least in part, why we did not see extra/ectopic hair follicles observed in *DKK2* or *Foxc2* null mice.

Increased FGF signaling in the Spry CKO eyelid epithelial cells did not inhibit conjunctival differentiation or induce a switch to epidermal fate such as those seen in FGFR2- or SMAD4-conditional null eyelids. A lack of decrease in BMP signaling in the Spry CKO

eyelids could be one reason for the continued maintenance of conjunctival cell fate. The results of Huang et al (2009) suggest broad roles for BMP signaling in regulation of epithelial proliferation, maintenance of the conjunctival differentiation program and peridermal migration. As a subset of these processes are also controlled by Spry-modulated FGF signaling, a critical goal of future studies would be to define the positive and negative feedback mechanisms that precisely control BMP and FGF signaling strengths in the eyelid primordia.

Supplementary Material

Refer to Web version on PubMed Central for supplementary material.

Acknowledgments

References

Ashery-Padan R, Marquardt T, Zhou X, Gruss P. Pax6 activity in the lens primordium is required for lens formation and for correct placement of a single retina in the eye. Genes Dev. 2000; 14:2701–11. [PubMed: 11069887]

Basson MA, Akbulut S, Watson-Johnson J, Simon R, Carroll TJ, Shakya R, Gross I, Martin GR, Lufkin T, McMahon AP, Wilson PD, Costantini FD, Mason IJ, Licht JD. Sprouty1 is a critical regulator of GDNF/RET-mediated kidney induction. Dev Cell. 2005; 8:229–39. [PubMed: 15691764]

Basson MA, Watson-Johnson J, Shakya R, Akbulut S, Hyink D, Costantini FD, Wilson PD, Mason IJ, Licht JD. Branching morphogenesis of the ureteric epithelium during kidney development is coordinated by the opposing functions of GDNF and Sprouty1. Dev Biol. 2006; 299:466–77. [PubMed: 17022962]

Chambers D, Mason I. Expression of sprouty2 during early development of the chick embryo is coincident with known sites of FGF signalling. Mech Dev. 2000; 91:361–4. [PubMed: 10704865]

Faedo A, Borello U, Rubenstein JL. Repression of Fgf signaling by sprouty1–2 regulates cortical patterning in two distinct regions and times. J Neurosci. 2010; 30:4015–23. [PubMed: 20237272]

Gage PJ, Qian M, Wu D, Rosenberg KI. The canonical Wnt signaling antagonist DKK2 is an essential effector of PITX2 function during normal eye development. Dev Biol. 2008; 317:310–24. [PubMed: 18367164]

Geh E, Meng Q, Mongan M, Wang J, Takatori A, Zheng Y, Puga A, Lang RA, Xia Y. Mitogen-activated protein kinase kinase kinase 1 (MAP3K1) integrates developmental signals for eyelid closure. Proc Natl Acad Sci U S A. 2011; 108:17349–54. [PubMed: 21969564]

Hanafusa H, Torii S, Yasunaga T, Nishida E. Sprouty1 and Sprouty2 provide a control mechanism for the Ras/MAPK signalling pathway. Nat Cell Biol. 2002; 4:850–8. [PubMed: 12402043]

Huang J, Dattilo LK, Rajagopal R, Liu Y, Kaartinen V, Mishina Y, Deng CX, Umans L, Zwijsen A, Roberts AB, Beebe DC. FGF-regulated BMP signaling is required for eyelid closure and to specify conjunctival epithelial cell fate. Development. 2009; 136:1741–50. [PubMed: 19369394]

Kawakami Y, Rodriguez-Leon J, Koth CM, Buscher D, Itoh T, Raya A, Ng JK, Esteban CR, Takahashi S, Henrique D, Schwarz MF, Asahara H, Izpisua Belmonte JC. MKP3 mediates the cellular response to FGF8 signalling in the vertebrate limb. Nat Cell Biol. 2003; 5:513–9. [PubMed: 12766772]

Klein OD, Minowada G, Peterkova R, Kangas A, Yu BD, Lesot H, Peterka M, Jernvall J, Martin GR. Sprouty genes control diastema tooth development via bidirectional antagonism of epithelial-mesenchymal FGF signaling. Dev Cell. 2006; 11:181–90. [PubMed: 16890158]

Kuracha MR, Burgess D, Siefker E, Cooper JT, Licht JD, Robinson ML, Govindarajan V. Spry1 and Spry2 are necessary for lens vesicle separation and corneal differentiation. Invest Ophthalmol Vis Sci. 2011; 52:6887–97. [PubMed: 21743007]

Li C, Guo H, Xu X, Weinberg W, Deng CX. Fibroblast growth factor receptor 2 (Fgfr2) plays an important role in eyelid and skin formation and patterning. Dev Dyn. 2001; 222:471–83. [PubMed: 11747081]

Li C, Scott DA, Hatch E, Tian X, Mansour SL. *Dusp6* (Mkp3) is a negative feedback regulator of FGF-stimulated ERK signaling during mouse development. Development. 2007; 134:167–76. [PubMed: 17164422]

Li G, Gustafson-Brown C, Hanks SK, Nason K, Arbeit JM, Pogliano K, Wisdom RM, Johnson RS. c-Jun is essential for organization of the epidermal leading edge. Dev Cell. 2003; 4:865–77. [PubMed: 12791271]

Luetteke NC, Phillips HK, Qiu TH, Copeland NG, Earp HS, Jenkins NA, Lee DC. The mouse waved-2 phenotype results from a point mutation in the EGF receptor tyrosine kinase. Genes Dev. 1994; 8:399–413. [PubMed: 8125255]

Luetteke NC, Qiu TH, Peiffer RL, Oliver P, Smithies O, Lee DC. TGF alpha deficiency results in hair follicle and eye abnormalities in targeted and waved-1 mice. Cell. 1993; 73:263–78. [PubMed: 8477445]

Miettinen PJ, Berger JE, Meneses J, Phung Y, Pedersen RA, Werb Z, Derynck R. Epithelial immaturity and multiorgan failure in mice lacking epidermal growth factor receptor. Nature. 1995; 376:337–41. [PubMed: 7630400]

Mine N, Iwamoto R, Mekada E. HB-EGF promotes epithelial cell migration in eyelid development. Development. 2005; 132:4317–26. [PubMed: 16141218]

Minowada G, Jarvis LA, Chi CL, Neubuser A, Sun X, Hacohen N, Krasnow MA, Martin GR. Vertebrate Sprouty genes are induced by FGF signaling and can cause chondrodysplasia when overexpressed. Development. 1999; 126:4465–75. [PubMed: 10498682]

Mukhopadhyay M, Gorivodsky M, Shtrom S, Grinberg A, Niehrs C, Morasso MI, Westphal H. Dkk2 plays an essential role in the corneal fate of the ocular surface epithelium. Development. 2006; 133:2149–54. [PubMed: 16672341]

Sharrocks AD. The ETS-domain transcription factor family. Nat Rev Mol Cell Biol. 2001; 2:827–37. [PubMed: 11715049]

Shim K, Minowada G, Coling DE, Martin GR. Sprouty2, a mouse deafness gene, regulates cell fate decisions in the auditory sensory epithelium by antagonizing FGF signaling. Dev Cell. 2005; 8:553–64. [PubMed: 15809037]

Smith RS, Zabaleta A, Kume T, Savinova OV, Kidson SH, Martin JE, Nishimura DY, Alward WL, Hogan BL, John SW. Haploinsufficiency of the transcription factors FOXC1 and FOXC2 results in aberrant ocular development. Hum Mol Genet. 2000; 9:1021–32. [PubMed: 10767326]

Swindell EC, Liu C, Shah R, Smith AN, Lang RA, Jamrich M. Eye formation in the absence of retina. Dev Biol. 2008; 322:56–64. [PubMed: 18675797]

Takatori A, Geh E, Chen L, Zhang L, Meller J, Xia Y. Differential transmission of MEKK1 morphogenetic signals by JNK1 and JNK2. Development. 2008; 135:23–32. [PubMed: 18032450]

Tao H, Shimizu M, Kusumoto R, Ono K, Noji S, Ohuchi H. A dual role of FGF10 in proliferation and coordinated migration of epithelial leading edge cells during mouse eyelid development. Development. 2005; 132:3217–30. [PubMed: 15958512]

Vassalli A, Matzuk MM, Gardner HA, Lee KF, Jaenisch R. Activin/inhibin beta B subunit gene disruption leads to defects in eyelid development and female reproduction. Genes Dev. 1994; 8:414–27. [PubMed: 8125256]

Zenz R, Scheuch H, Martin P, Frank C, Eferl R, Kenner L, Sibilia M, Wagner EF. c-Jun regulates eyelid closure and skin tumor development through EGFR signaling. Dev Cell. 2003; 4:879–89. [PubMed: 12791272]

Zhang L, Wang W, Hayashi Y, Jester JV, Birk DE, Gao M, Liu CY, Kao WW, Karin M, Xia Y. A role for MEK kinase 1 in TGF-beta/activin-induced epithelium movement and embryonic eyelid closure. Embo J. 2003; 22:4443–54. [PubMed: 12941696]

Highlights

- Sprys are downstream targets and negative modulators of the FGF signaling pathway

- Conjunctival epithelial cells express *Spry1* and *Spry2* during eyelid closure

- Deletion of *Spry1* and *Spry2* in the ocular surface epithelium inhibits eyelid closure

- *Spry1* and *Spry2* regulate peridermal motility through c-Jun but not ERK

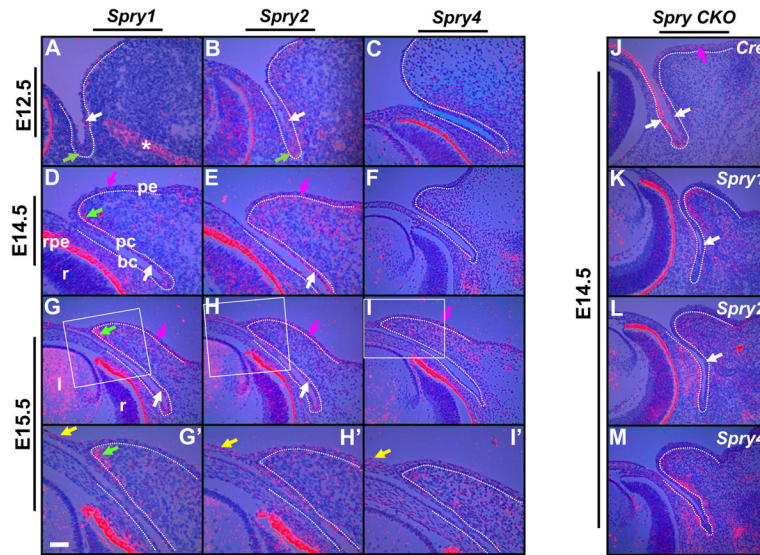- *Spry1* and *Spry2* suppress conjunctival proliferation through FGF-ERK signaling

Figure 1.
Spry 1, *Spry2* and *Spry4* expression in wildtype and Spry CKO mutant eyelids. ^{35}S-labeled *Spry1* (A, D, G, G′, K), *Spry2* (B, E, H, H′, L), *Spry4* (C, F, I, I′, M) and Cre (J) riboprobes were hybridized to sections of E12.5 (A, B, C), E14.5 (D, E, F) and E15.5 (G–I′) wildtype and E14.5 (J–M) Spry CKO mutant embryos. The dotted lines delineate the boundary between the epithelial and mesenchymal cells. G′–I′ are higher magnifications of boxed regions in G–I. Conjunctival epithelial cells expressed *Spry1* (A, D, G, white arrows) and *Spry2* (B, E, H, white arrows), the palpebral epidermal cells expressed *Spry1* (D, G, magenta arrows), *Spry2* (E, H, magenta arrows) and *Spry4* (I, magenta arrow) and the eyelid mesenchymal cells showed localized expression of Spry1 (D, G, G′, green arrows) but broader expression of *Spry2* (E, H, H′) and *Spry4* (F, I, I′). Peridermal cells expressed all three *Sprys* (G′–I′, yellow arrows). In the Spry CKO eyelids, the conjunctival epithelial cells expressed *Cre* recombinase (J, white arrows) and showed near complete loss of *Spry1* (K, white arrow) and *Spry2* (L, white arrow) expression. The eyelid mesenchymal cells showed increased expression of *Spry1* (compare K to D) and *Spry 4* (compare M to F) and the bulbar mesenchymal cells showed increased expression of *Spry2* (compare L to E) and *Spry4* (compare M and F. Asterisk in panel A marks *Spry1* expression in the nasolacrimal duct. Staining in the retinal pigmented epithelium (D, rpe) is an artifact of dark-field illumination. Abbreviations; bc, bulbar conjunctiva; l, lens; pc, palpebral conjunctiva; pe, palpebral epidermis; r, retina. Scale bar in (G′): (A, B, C, G′–I′) 50 μm; (D–I, J–M) 100 μm.
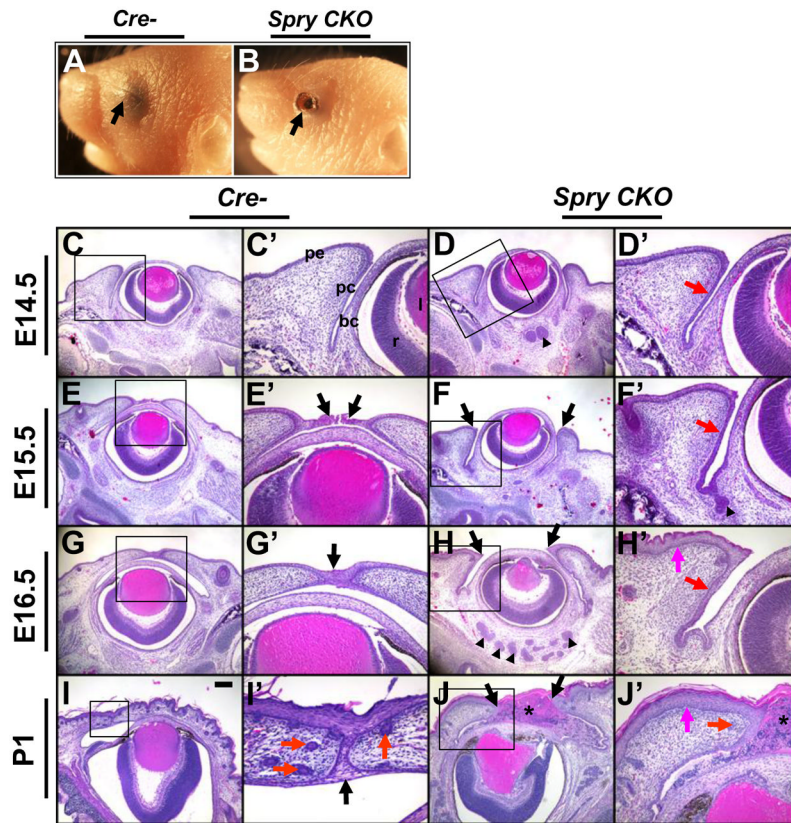
Figure 2.
Spry CKO mutants are born with open eyelids. New born Spry CKO pups display the 'EOB' phenotype (B, arrow) in contrast to Cre- control (A) littermates. Frontal sections of E14.5 (C–D′), E15.5 (E–F′), E16.5 (G–H′) and P1 (I–J′) of Cre- and Spry CKO embryos were stained with hematoxylin and eosin. C′–J′ are higher magnifications of boxed regions in C–J. Spry CKO palpebral conjunctival epithelium (D′, F′, H′, red arrow) and palpebral peridermis (H′, J′, magenta arrow) were hyperplastic. Margins of the upper and lower eyelids in the Spry CKO embryos (F–J, black arrows) remained unfused in contrast to Cre-littermates (E′, G′, I′, arrows). Red arrows in I′ and J′ mark hair follicles. Asterisk in J marks inflammatory infiltrates between the two eyelids. Abbreviations; bc, bulbar conjunctiva; l, lens; pc, palpebral conjunctiva; pe, palpebral epidermis; r, retina. Scale bar in (I): (A, B) 1 mm; (C–J) 200 μm; (I′) 40 μm; (C′–H′, J′) 80 μm.
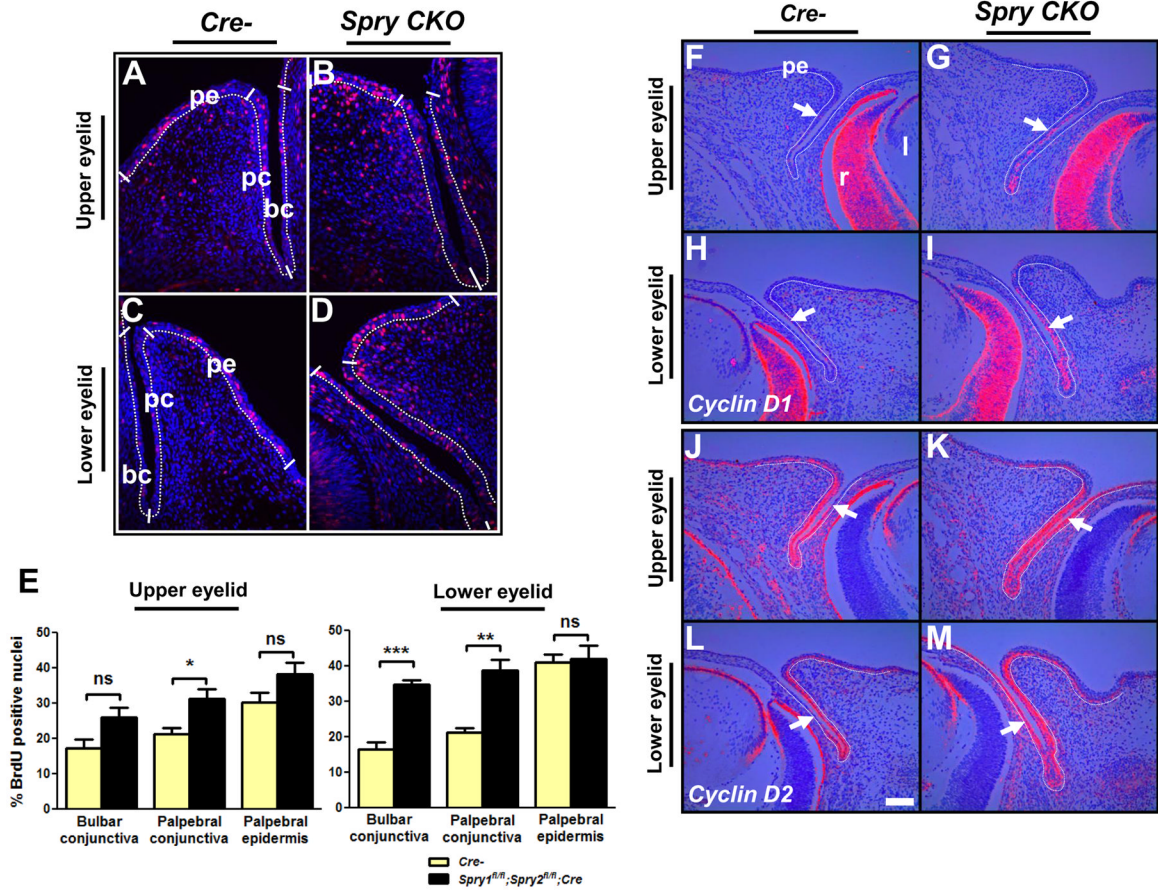
Figure 3.
Increased epithelial proliferation in Spry CKO eyelids. Cell proliferation in E14.5 Cre- (A, C) and Spry CKO (B, D) eyelids was assessed by a BrdU incorporation assay and the BrdU labeling index was quantified (E). Palpebral cojunctival epithelial cells of lower and upper eyelids and bulbar conjunctival epithelial cells of lower eyelids showed significant increases in proliferation. Error bars, SEM. ^{35}S-labeled *cyclin D1* (F–I) and *cyclin D2* (J–M) riboprobes were hybridized to sections of E14.5 Cre- and Spry CKO mutant embryos. The dotted lines delineate the boundary between the epithelial and mesenchymal cells. *Cyclin D1* levels were increased in the palpebral conjunctival cells of upper (G, arrow) and lower (I, arrow) eyelids. *Cyclin D2* levels were increased in the bulbar conjunctival cells of upper (K, arrow) and lower (M, arrow) eyelids. Abbreviations; bc, bulbar conjunctiva; l, lens; pc, palpebral conjunctiva; pe, palpebral epidermis; r, retina. Scale bar in (L): (A–D) 50 μm; (F–M) 100 μm.
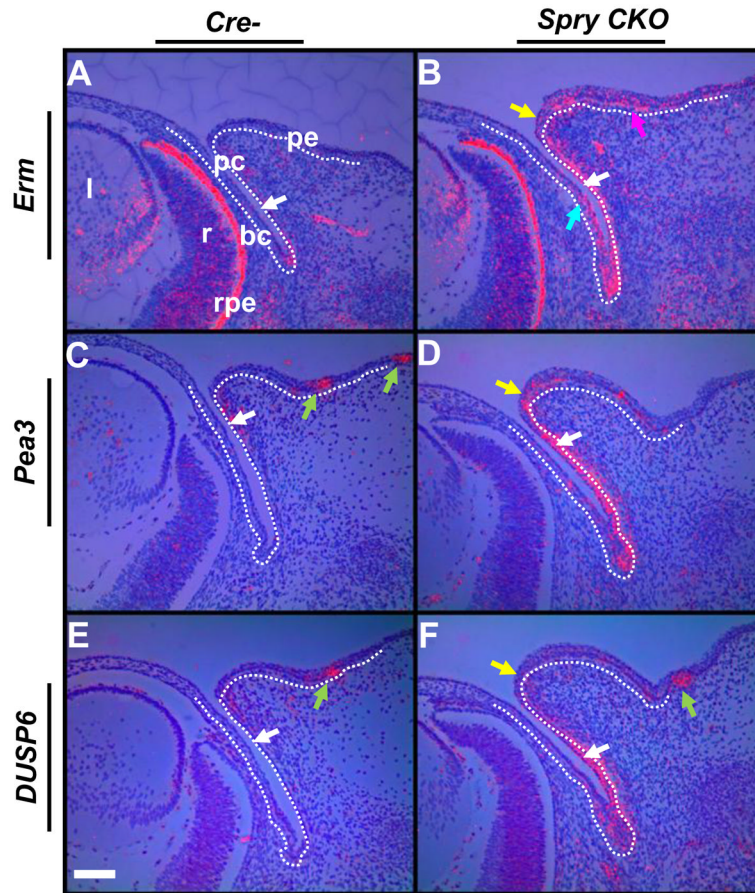
Figure 4.
Induction of FGF signaling targets in Spry CKO eyelids. ^{35}S-labeled *Erm* (A, B), *Pea3* (C, D) and *Dusp6* (E, F) riboprobes were hybridized to sections of E14.5 Cre- and Spry CKO mutant embryos. The dotted lines delineate the boundary between the epithelial and mesenchymal cells. *Erm*, *Pea3* and *Dusp6* were induced in the palpebral conjunctival cells (B–F, white arrows) and peridermal cells (B, D, F, yellow arrow). Erm was also induced in the palpebral epidermis (B, magenta arrow). Green arrows mark expression of *Pea3* (C) and *Dusp6* (E, F) in the hair follicles of the skin. Staining in the retinal pigmented epithelium (D, rpe) is an artifact of dark-field illumination. Abbreviations; bc, bulbar conjunctiva; l, lens; pc, palpebral conjunctiva; pe, palpebral epidermis; r, retina. Scale bar in (E): (A–F) 100 μm.
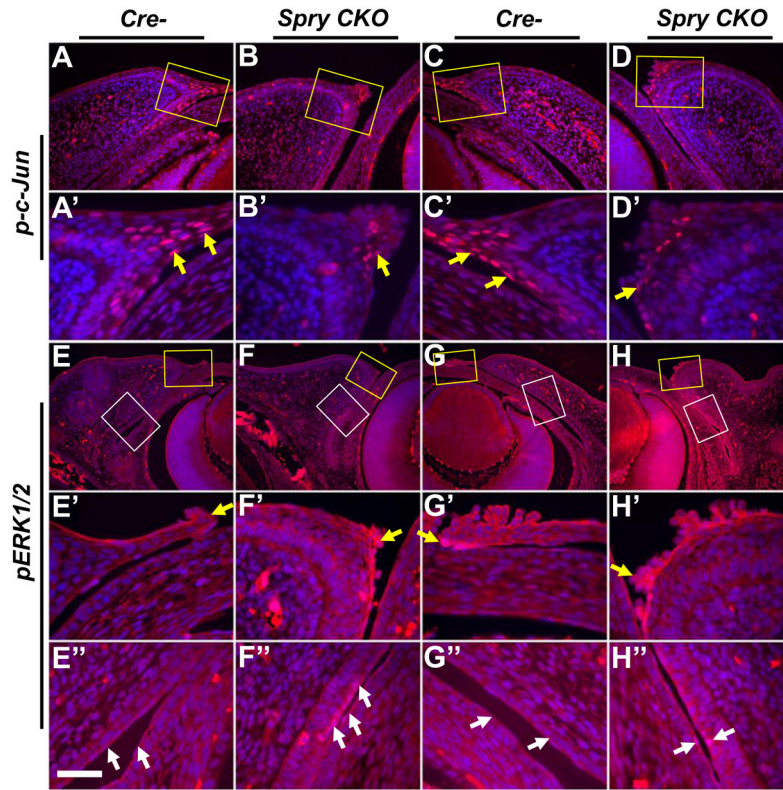
Figure 5.
ERK and c-Jun phosphorylation in Spry CKO eyelids. Alterations in ERK and c-Jun phosphorylation in E14.5 Cre- and Spry CKO eyelids were analyzed immunohistochemistry. Upper eyelids are shown in panels A–B′, E–F″ and lower eyelids are shown in panels C–D′, G–H″. A′–H′ are higher magnifications of anterior margins (yellow squares) in panels A–H. E″–H″ are higher magnifications of conjunctiva (white squares) in E–H. c-Jun phosphorylation is reduced in the peridermal cells at the leading edge of Spry CKO upper (B′, arrow) and lower (D′, arrow) eyelids. ERK phosphorylation in the Spry CKO eyelids (F′, H′) remained unaltered in the peridermal cells. In contrast, conjunctival epithelial cells of Spry CKO upper (F″, arrows) and lower (H″, arrows) lids showed increased ERK phosphorylation. Scale bar in (E″): (A–D) 120 μm; (A′–D′) 40 μm; (E–H) 240 μm; (E′–H″) 40 μm.

Figure 6.
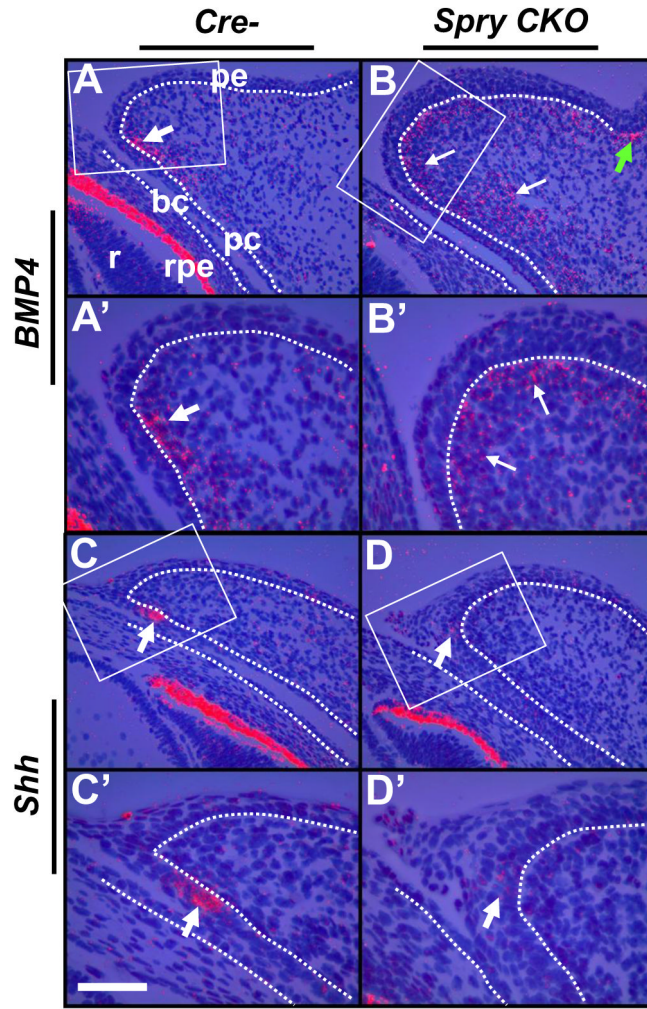*Shh* and *BMP4* expression in Spry CKO eyelids. ^{35}S-labeled BMP4 (A–B′) and Shh (C–D′) riboprobes were hybridized to sections of E14.5 Cre- and Spry CKO mutant embryos. The dotted lines delineate the boundary between the epithelial and mesenchymal cells. A′–D′ are higher magnifications of boxed regions in A–D. *BMP4*-positive mesenchymal cells in Spry CKO eyelids were clustered near the anterior margin (A, A′, white arrows) but appeared disaggregated in Cre- eyelids (B, B′, white arrows). Conjunctival epithelial cells at the margin showed reduced expression of *Shh* (compare D and D′ to C and C′ respectively). Green arrows in B and B′ mark *BMP4* expression in the hair follicles of the skin. Staining in the retinal pigmented epithelium (rpe) is an artifact of dark-field illumination. Abbreviations; bc, bulbar conjunctiva; l, lens; pc, palpebral conjunctiva; pe, palpebral epidermis; r, retina. Scale bar in (C′): (A–B′, C, D) 100 μm; (C′–D′) 50 μm.
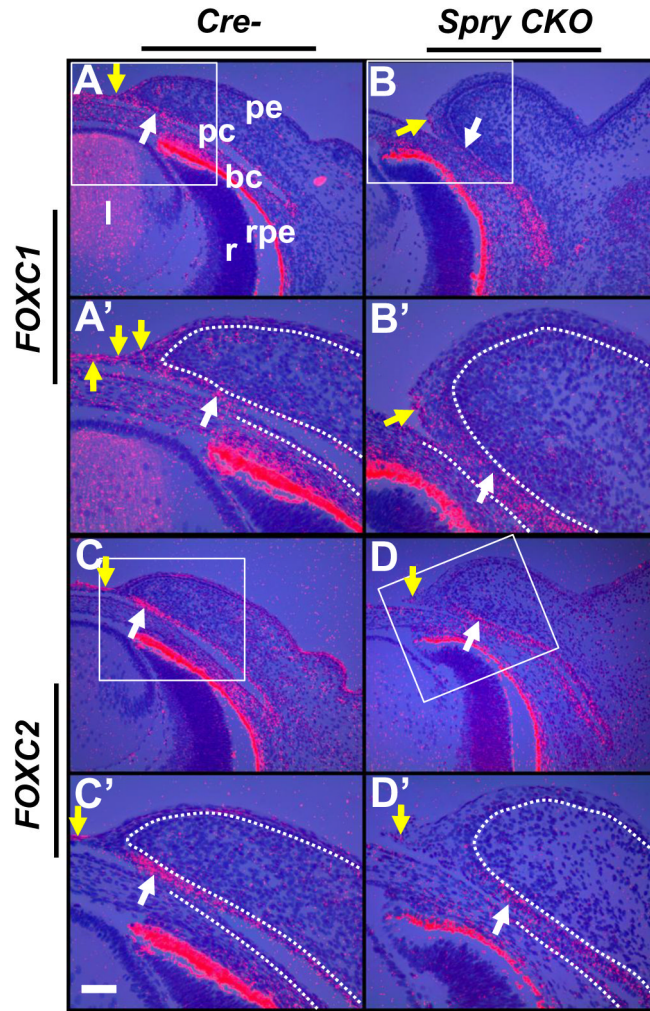
Figure 7.
Foxc1 and *Foxc2* expression in Spry CKO eyelids. ^{35}S-labeled *Foxc1* (A–B′) and *Foxc2* (C–D′) riboprobes were hybridized to sections of E14.5 Cre- and Spry CKO mutant embryos. The dotted lines delineate the boundary between the epithelial and mesenchymal cells. A′–D′ are higher magnifications of boxed regions in A–D. Modest reduction in *Foxc1* (B, B′) and a strong reduction in *Foxc2* (D, D′) was seen at the anterior margins of Spry CKO eyelids when compared to Cre- eyelids (B, B′, white arrows). Spry CKO peridermal cells also showed reduced expression of *Foxc1* (B′, yellow arrow) and *Foxc2* (D, D′, yellow arrow) compared to Cre- eyelids (A, A′, C, C′, yellow arrows). Staining in the retinal pigmented epithelium (rpe) is an artifact of dark-field illumination. Abbreviations; bc, bulbar conjunctiva; l, lens; pc, palpebral conjunctiva; pe, palpebral epidermis; r, retina. Scale bar in (C′): (A–D) 100 μm; (A′–D′) 50 μm.
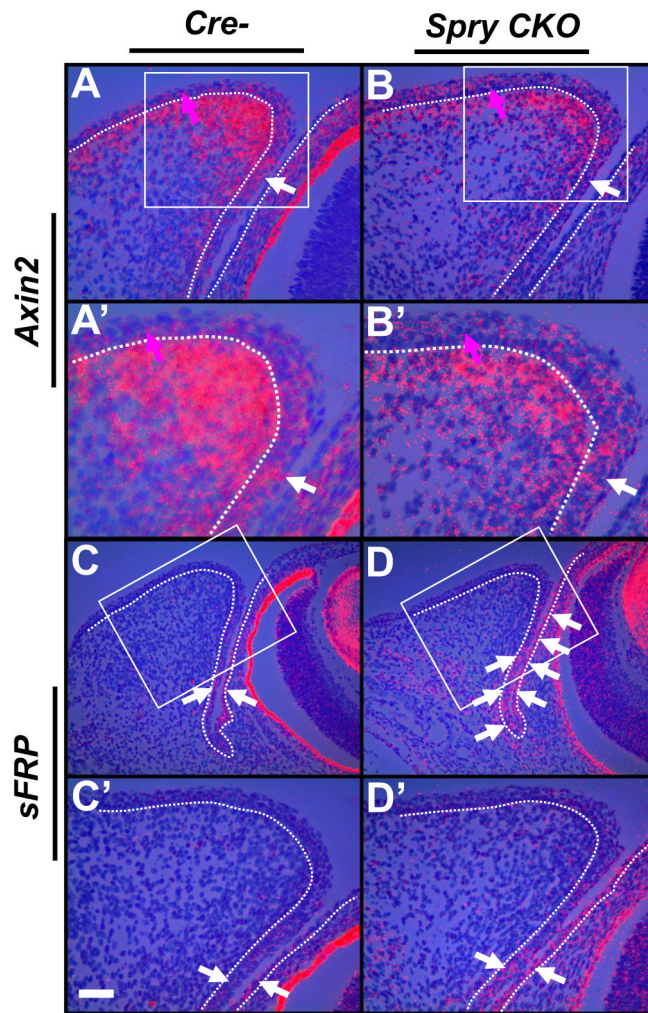
Figure 8.
Decreased Wnt signaling in Spry CKO eyelids. ^{35}S-labeled *Axin2* (A–B′) and *sFRP1* (C–D′) riboprobes were hybridized to sections of E14.5 Cre- and Spry CKO mutant embryos. The dotted lines delineate the boundary between the epithelial and mesenchymal cells. A′–D′ are higher magnifications of boxed regions in A–D. *Axin2* (B, B′) expression was modestly reduced in the Spry CKO conjunctival epithelial cells (B, white arrow) and in eyelid mesenchymal cells (A, B) but was not in the palpebral peridermal cells (B, magenta arrows). *sFRP1* was increased in the Spry CKO conjunctival epithelial cells (D, D′, white arrows). Staining in the retinal pigmented epithelium (rpe) is an artifact of dark-field illumination. Abbreviations; bc, bulbar conjunctiva; l, lens; pc, palpebral conjunctiva; pe, palpebral epidermis; r, retina. Scale bar in (C′): (A, B, A′, B′, C′, D′) 50 µm; (C, D) 100 µm.
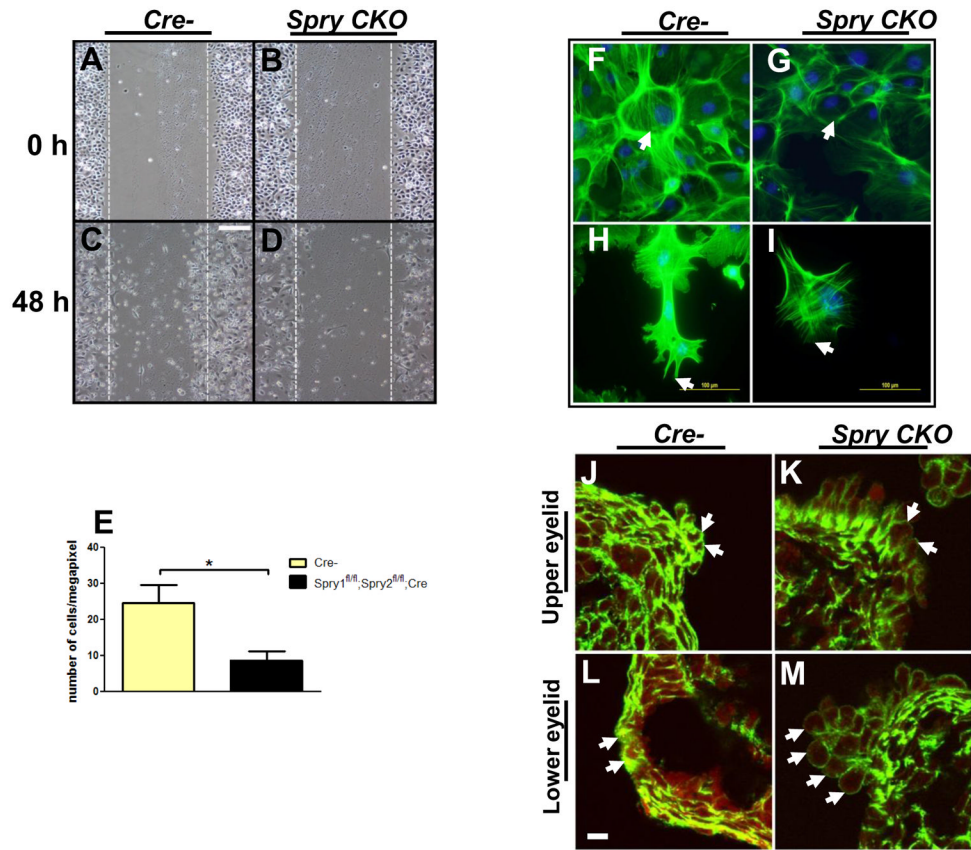
Figure 9.
Reduced motility of Spry CKO eyelid epithelial cells. A–E. A reduced number of Spry CKO eyelid keratinocytes (D, E) migrated into the gap (A–D, circumscribed by dotted lines) 48 hours after a scratch was made on monolayered cultures of Spry CKO and Cre- eyelid keratinocytes. F–I. Phalloidin staining showed reduced F actin in Spry CKO eyelid keratinocytes with reduced stress fibers (G, white arrows) and thinner filipodia (I, arrow). J–M. Phalloidin staining showed reduced F actin in the peridermal cells at the leading edge of Spry CKO eyelids (K, M, arrows). Scale bar in (A–D) 100 µm; (F, G) 200 µm; (H,I) 100 µm; (J–M) 5 µm.
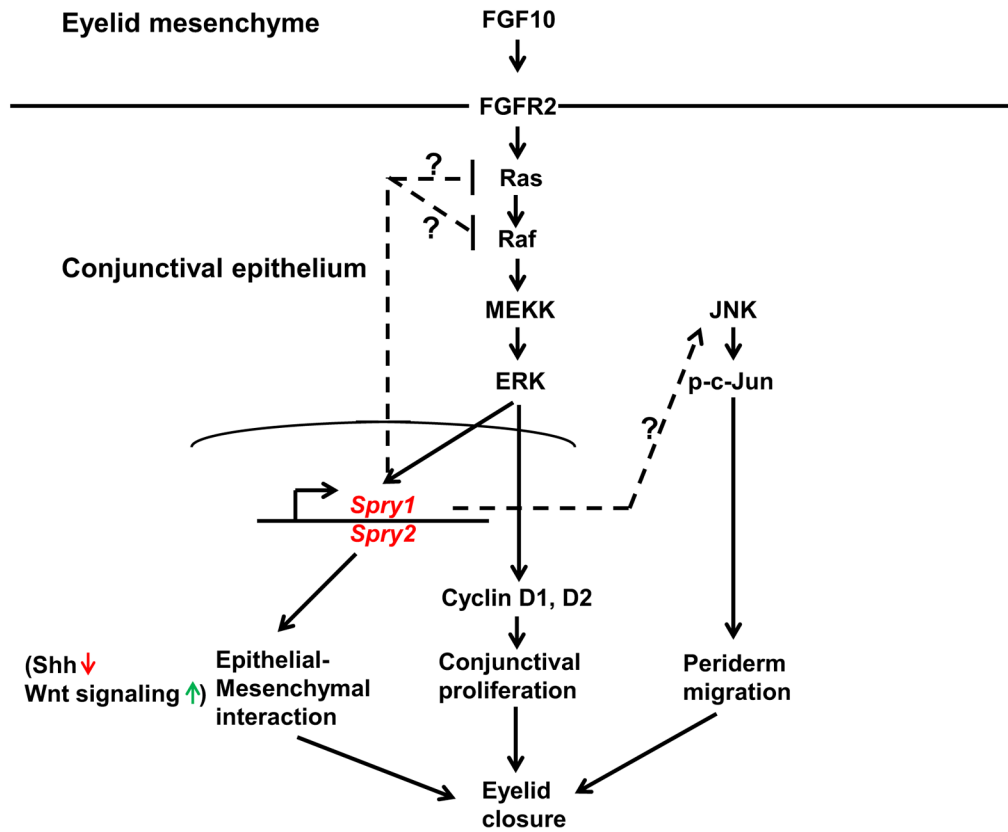
Figure 10.
Proposed functions of Spry1 and Spry2 in regulation of eyelid closure. Spry1 and Spry2 a) redundantly and negatively modulate FGF signaling in the conjunctival epithelial cells to suppress cell proliferation, b) mediate eyelid epithelial-mesenchymal communication (reflected by reduced Shh and increased Wnt signaling in Spry CKO eyelids) and c) regulate peridermal cell motility (ERK-independent modulation of phospho-c-Jun levels and F actin polymerization). The FGF signaling pathway modulated by Sprys is likely to be initiated by FGF10 from the eyelid mesenchyme.